

# High Precision Positioning of a Mechanism With Nonlinear Friction Using a Fuzzy Logic Pulse Controller\*

M.R. Popović<sup>†</sup>, D.M. Gorinevsky<sup>‡</sup>, and A.A. Goldenberg

Robotics and Automation Laboratory, University of Toronto  
5 King's College Rd., Toronto, Ontario M5S 3G8, CANADA  
e-mail: popovic@aut.ee.ethz.ch

## Abstract

*A new approach to very accurate positioning of mechanical devices with nonlinear (stick-slip) friction is presented in this paper. The proposed controller applies narrow torque pulses to move a mechanism to a desired position despite nonlinear friction. The pulse shapes generated by the controller are computed using a fuzzy logic approximation of the dependence between the desired displacement and the torque pulse shape. The closed-loop stability conditions for the proposed controller are derived taking into consideration a random variation of friction. A detailed experimental study of the system response to different torque pulse shapes and a detailed controller design are presented for a direct-drive mechanism. In the experiments it was demonstrated that the proposed controller achieves positioning accuracy which is within the limits of the position encoder resolution.*

## 1 Introduction

Very accurate positioning is required in mechanical devices such as surgical tools, computer disk drives, assembly robots, micro-mechanisms, etc. For many of these devices, the performance is limited by friction-caused positioning errors. Precise positioning, in particular, control of very small displacements is an especially difficult problem for direct-drive mechanisms. These devices have no transmission between the drive and the output motion. The

---

\*Supported by a grant from MRCO, Ontario, Canada

<sup>†</sup>Currently with Automatic Control Laboratory, Swiss Federal Institute of Technology Zurich - ETH Zurich, ETH Zentrum / ETL I24.2, CH-8092 Zurich, Switzerland

<sup>‡</sup>Currently with Honeywell Technology Center, Honeywell CA35-5272H, One Results Way, Cupertino, CA 95014, USA

absence of a transmission mechanism combined with the existence of nonlinear (stick-slip) friction often creates problems with precise positioning.

A number of control strategies has been developed to overcome the problems caused by the stick-slip effect. The most relevant published strategies are: friction compensation using dither signal [1]; friction compensation through position or force control using high gain feedback [2]; adaptive feedback friction compensation [3]; robust nonlinear friction compensation [9, 14, 17]; model-based feed-forward friction compensation [1, 11]; and precise positioning using pulse control [7, 8, 16]. Among them, the last two groups of methods are particularly effective in performing very accurate positioning.

Short force pulses were used for precise positioning of mechanical devices by Yang and Tomizuka [16], Higuchi and Hojjat [7, 8], and Armstrong [1]. In [7, 8] as well as in [16] simple models of friction are used to calculate the amplitude or the duration of the applied force pulse<sup>1</sup> as a function of the desired displacement. Such models do not take into account the nonlinearity of friction, in particular, the negative damping friction which causes the stick-slip effect. As a result, the two methods are not best suited for controlling very small displacements where nonlinear friction properties are strongly manifested<sup>2</sup>. On the other hand, Armstrong [1] uses a detailed friction model in the form of a look-up table to calculate force pulses as a function of the desired displacement. The main problem with this method is that it requires large computer memory for storing the look-up table, and extensive experimentation to fill up the table [1].

This paper proposes a novel design of a torque-pulse controller that is well suited to work in the presence of nonlinear friction and, unlike Armstrong's method, does not require massive data storage. Also, unlike the strategies of [1, 7, 16], this controller has the flexibility of selecting different pulse shapes depending on the displacement that needs to be performed. The proposed fuzzy logic controller should be enacted after a conventional controller brings the mechanism to the vicinity of a desired position, in order to further reduce the steady-state position error of the conventional controller. The proposed approach is rather general

---

<sup>1</sup>The authors modeled dependence of only one torque pulse parameter as a function of desired displacement, while the second parameter was kept constant. For example, Yang and Tomizuka used the duration of the rectangular torque pulse to control the displacement.

<sup>2</sup>Term "very small displacements" is used to describe displacements for which average velocity of the pulse-controlled mechanism is within the nonlinear friction range. Particular dimensions of "very small displacement" and the impact of friction nonlinearity on the mechanism can vary substantially depending on the application.

and requires a minimum of device-dependent data. Experiments conducted with a direct-drive mechanism have demonstrated that the proposed controller improves the positioning accuracy of the system up to the encoder resolution limit<sup>3</sup>, which is more than an order of magnitude better than the accuracy obtained with a PID controller. The control strategy used in this paper is related to the approximation-based feed-forward control method in [4, 5]. The conference version of this paper is in [12].

The organization of the paper is as follows. Section 2 defines the control problem addressed. The controller design is presented in Section 3 and the experiments with the direct-drive mechanism are described in Section 4. Conclusions are given in Section 5.

## 2 Control Problem

### 2.1 Modeling the Response to Short Torque Pulses

Let us first consider the response of a mechanism with friction to narrow open-loop torque pulses. The model presented herein is the result of extensive experimentation described in [13], which is also partially discussed in Section 4. The proposed empirical model is well suited for the design and analysis of pulse controllers for mechanisms with friction. The controller design presented in this paper is based on this model.

Let us now discuss the motion of the mechanism under the influence of a torque pulse. In particular, consider a rectangular torque pulse that can be defined as  $Q(t) = A$  for  $0 \leq t < \tau$  and  $Q(t) = 0$  for  $t \geq \tau$ , where  $Q$  denotes the torque,  $A$  denotes the pulse amplitude,  $\tau$  denotes the pulse duration and  $t$  denotes the time after the controller engagement. This paper also considers more general pulse shapes with bounded amplitude and duration implementable with a digital controller. Let us now denote by  $\Delta\theta$  the difference between initial ( $t = 0$ ) and final ( $t \geq T$ ) steady-state positions of the mechanism obtained after a torque pulse has been applied to it. The dependence of the steady-state displacement  $\Delta\theta$  on the pulse shape  $Q(\cdot)$  can be presented in the following operator form:

$$\Delta\theta = F[Q(\cdot)], \tag{1}$$

---

<sup>3</sup>If the encoder measures displacements with accuracy  $10^{-5}$  m or lower, then the PID controller can position the mechanisms with one encoder increment resolution. If the encoder can measure displacements smaller than  $10^{-6}$  m (what is our case) then the positioning with the encoder resolution cannot be achieved. The main obstacle in achieving higher positioning precision is random friction, generated by the surface asperities, which is position dependent and changes every  $10^{-7}$  m [1, 11, 12].

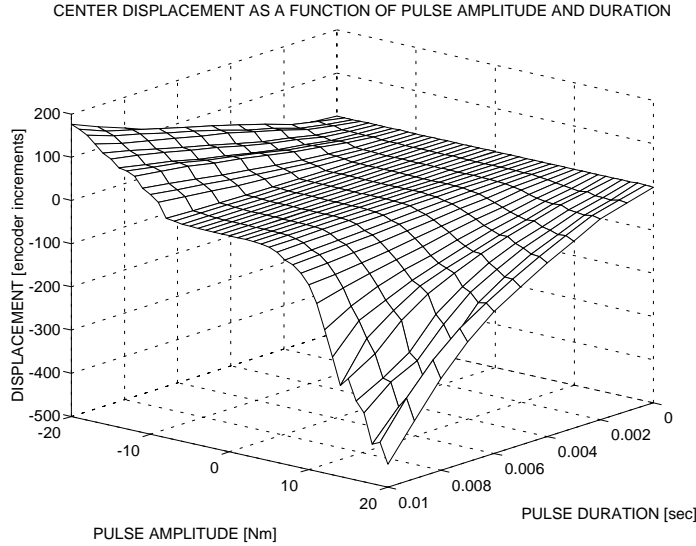


Figure 1: Experimentally obtained center displacement  $\Delta\theta_{ctr}$  of the experimental mechanism as a function of pulse amplitude  $A$  and pulse duration  $\tau$ .

where  $Q(\cdot)$  denotes the overall pulse shape as a function of time  $Q(t)$ ,  $t \in [0, T]$  and not its instantaneous value; and  $F[Q(\cdot)]$  denotes a nonlinear operator that defines the displacement  $\Delta\theta$  for the torque pulse  $Q(\cdot)$ . The equation (1) is written under the assumption that the mechanism displacement does not depend on its initial position. This is true in most cases, in particular for the experimental mechanism described in Section 4. Another assumption implicitly made in the above formulation is that gravity and other external forces which act on the mechanism are compensated for. In other words, the pulse torque is added to a compensating torque and is used only to move the mechanism from one steady-state position to another. The compensating torque ensures that the mechanism remains at the steady-state position thereafter.

For the special case where the torque pulse  $Q(\cdot)$  is a rectangular torque pulse, the relationship (1) can be represented in the following form:

$$\Delta\theta = F[Q(\cdot)] = \Phi(A, \tau), \quad (2)$$

where  $\Phi(A, \tau)$  describes the dependence of the mechanism steady-state displacement on the amplitude  $A$  and duration  $\tau$  of the rectangular torque pulse. Figure 1 illustrates the function  $\Phi(A, \tau)$  obtained for the experimental setup discussed in Section 4. Note that the experimentally obtained dependence of  $\Phi(A, \tau)$  in Figure 1 has some local deviations from monotonicity that are caused by the random variation of the measured displacements.

It is well known from the literature [1, 11], and it was also confirmed by our experiments

described in [13], that low velocity friction contains a significant random component. If the random friction component and measurement errors are taken into consideration, models (1) and (2) hold only statistically. In fact, (1) and (2) should be represented as:

$$\Delta\theta = F[Q(\cdot)] + \epsilon_1, \quad (3)$$

where  $\epsilon_1$  describes the combined influence of random friction torque and position measurement error. The experiments in [13] have shown that the random variable  $\epsilon_1$ , generated by short torque pulses, is a bounded random variable which decreases with displacement  $\Delta\theta$ . In particular, it was found out that  $|\epsilon_1| \leq \xi|\Delta\theta|$ , where  $\xi$  ( $0 < \xi < 1$ ) is an empirical parameter. This inequality is discussed in more details later on in this paper.

## 2.2 Problem Statement

The controller proposed in this paper should be used after a conventional controller brings the system to the vicinity of a desired position and should operate as follows. First, a difference between the desired and the actual positions of the system is determined. Second, a shape of the pulse is calculated as a function of this difference. After sending the calculated torque pulse to the motor, the controller waits until a new steady-state of the mechanism is reached. If the difference between the newly measured and the desired position is outside the bounds of the required precision, a new control cycle is initiated.

The proposed controller is a deadbeat sampled-data controller. Once the torque pulse is calculated by the controller, the controller does not have any influence on the system behaviour until a new sample command is issued. Between sampling instances the system behaves as an open-loop system. Friction, which acts as a braking device and limits the motion of the mechanical systems, ensures that the motion between the sampling instances is always bounded. This is an interesting concept, because the proposed controller is overcoming problems induced by low velocity friction, and at the same time uses the friction to ensure that the mechanism settles down during the sampling period.

Let us now formulate the controller design problem in a more formal way. The pulse controller is defined by a two-argument function  $\Psi(t; \Delta\theta_d)$ , which gives the time dependence of the motor torque (pulse shape) for a given desired displacement of the mechanism  $\Delta\theta_d$ . For each desired displacement  $\Delta\theta_d$  within given bounds  $|\Delta\theta_d| \leq \Theta_*$  ( $\Theta_*$  is the maximum

displacement the controller is designed to perform), the controller computes a pulse shape:

$$\Psi(t ; \Delta\theta_d) = Q(t), \quad (4)$$

where the time  $t$  is defined on the interval  $[0, T]$ . Ideally, the controller (4) should be designed in such a way that in the absence of disturbances the displacement caused by the torque pulse (4) is exactly the desired displacement  $\Delta\theta_d$ . In reality, due to its computational inaccuracy the controller (4) may cause a displacement different from the desired one even when there are no disturbances affecting the system ( $\epsilon_1 = 0$ ):

$$F[\Psi(\cdot ; \Delta\theta_d)] = \Delta\theta_d + \epsilon_2, \quad (5)$$

where  $\epsilon_2$  denotes the position error caused by the computational inaccuracy of the controller.

Let us denote by  $\theta_d$  the desired position and by  $\theta_n$  the measured position at the control cycle  $n$ . In accordance with (3) and (5), the position of the mechanism at the control cycle  $n + 1$  is given by the following expression:

$$\theta_{n+1} = F[\Psi(\cdot ; (\theta_d - \theta_n))] + \theta_n + \epsilon_{1_n} + \epsilon_{2_n}, \quad (6)$$

where  $\epsilon_{1_n}$  is the displacement error at the control cycle  $n$  caused by the random friction and measurement errors (as in (3)), and  $\epsilon_{2_n}$  is a computational error at the control cycle  $n$  caused by the controller design (as in (5)). Expression (6) describes the model of the closed-loop system, which is schematically presented in Figure 2.

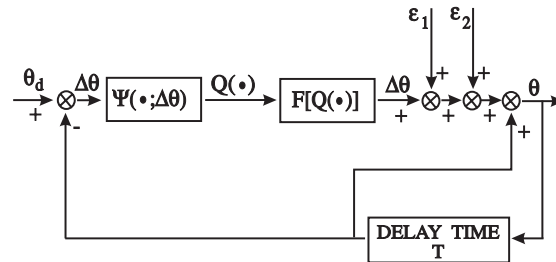


Figure 2: Schematic diagram of the closed-loop system

### 2.3 Stability Conditions

In order for the closed-loop system (6) to converge to the desired position  $\theta_d$ , it must be proved that there exists a number of consecutive torque pulses  $N$  such that for all  $n \geq N$

$|\theta_n - \theta_d| < \Delta$ , where  $\Delta$  is the error deadzone. Such convergence conditions are provided by the following Theorem:

**Theorem 2.1** *Consider a pulse controller defined by mapping  $\Delta\theta_d \mapsto \Psi(\cdot ; \Delta\theta_d)$ , where  $\Delta\theta_d \in [-\Theta_*, \Theta_*]$  is the difference between the desired position and the measured position of the mechanism and  $\Psi(\cdot ; \Delta\theta_d)$  is the pulse generated by the controller for given desired displacement  $\Delta\theta_d$ . Assume that the controller is designed to satisfy (5) and consider the closed-loop system given by (6):*

$$\theta_{n+1} = F[\Psi(\cdot, (\theta_d - \theta_n))] + \theta_n + \epsilon_{1n} = \theta_d + \epsilon_{1n} + \epsilon_{2n} \quad (7)$$

where  $\epsilon_{1n}$  is the random displacement variation at control step  $n$  and  $\epsilon_{2n}$  is the controller error at control step  $n$ . Then, the closed-loop system (7) satisfies the inequality:

$$|\theta_d - \theta_{n+1}| < \alpha^n |\theta_d - \theta_1| \quad (8)$$

as long as the following (controller dependent) conditions hold:

$$|\epsilon_{1n}| < \beta_1 |\theta_d - \theta_n|, \quad |\epsilon_{2n}| < \beta_2 |\theta_d - \theta_n|, \quad \beta_1 + \beta_2 = \alpha < 1 \quad (9)$$

**Proof:** is straightforward and can be found in [12]. □.

In practical applications, one is faced with a problem of controlling displacements which are of the same order of magnitude as the measurement error. Conditions (9) are never satisfied for very small displacements, such as single encoder increment displacement, because the relative measurement error is large. Therefore, for practical applications the following corollary of Theorem 2.1 can be used:

**Corollary 2.1** *Let the convergence conditions of Theorem 2.1 hold for  $|\Delta\theta_d| > \Delta_o$ . Consider a dead-zone controller  $\Psi(\cdot ; \Delta\theta_d)$  that has a zero output for  $|\Delta\theta_d| \leq \Delta_o$ . Then the difference between the desired position and the measured position of the mechanism  $|\theta_d - \theta_n|$  will be brought within the deadzone  $\Delta_o$  after at most  $n_o = \text{Integer}[(\ln \Delta_o - \ln |\theta_d - \theta_1|) / \ln(\alpha)] + 1$  control cycles.*

**Proof:** From (8) it can be shown that  $|\theta_d - \theta_{n_o+1}| < \alpha^{n_o} |\theta_d - \theta_1|$  and from  $n_o = \text{Integer}[(\ln \Delta_o - \ln |\theta_d - \theta_1|) / \ln(\alpha)] + 1$  follows that  $\alpha^{n_o} |\theta_d - \theta_1| < \Delta_o$ . Hence,  $|\theta_d - \theta_{n_o+1}| < \Delta_o$ . □.

### 3 Fuzzy Logic Controller

The proposed controller is defined by the function  $\Psi(\cdot; \Delta\theta)$  in (4). The practical requirements for the controller design are as follows: simplicity; minimal time and knowledge required to design the controller; and closed-loop convergence conditions given by Theorem 2.1. A conceptual framework that conveniently satisfies all of the above considerations is given by the fuzzy-logic approach, which is simple and accessible to practitioners.

The controller (4) is designed based on the model of the form (2). The system's response (2) to rectangular torque pulses (see Figure 1) and the properties of mechanism's random friction are identified experimentally. The following guidelines for conducting such experiments are suggested:

- Select the rectangular torque pulses such that the displacements caused by these pulses cover the range  $[-\Theta_*, \Theta_*]$ , where  $\Theta_*$  is the maximum displacement the controller is designed to compensate for.
- For controlling small displacements it is better to use short torque pulses, because shorter pulses provide better positioning accuracy, as shown in Figure 1.
- For larger displacements, a duration of the rectangular torque pulse  $\tau$  should be selected in such a way that the pulse with maximum acceptable amplitude and duration  $\tau$  causes a displacement larger than the maximum displacement  $\Theta_*$  the controller is expected to perform.

In addition to the displacement, the experimental data is used to estimate statistical parameters of the displacements, such as: displacement's upper bound  $\Delta\theta_{max}$ , displacement's lower bound  $\Delta\theta_{min}$  and displacement's center of distribution  $\Delta\theta_{ctr}$  [6, pages 74–112]. In order to obtain these statistical parameters, exploratory experiments for each pulse shape had to be repeated several times. Once obtained, these parameters are plotted as a function of the pulse amplitude  $A$  and the pulse duration  $\tau$  (see Figures 1 and 6).

Let us now assume that the controller designed herein will generate control pulses with error  $\epsilon_2$  in (5). If we take into consideration random displacement variation  $\epsilon_1$ , in (3), then the controller (5) will cause the mechanism to perform “total displacement”  $\Delta\theta$ , such that  $\Delta\theta - \Delta\theta_d = \epsilon_1 + \epsilon_2$ . Since  $|\epsilon_1| \leq |\Delta\theta_{max} - \Delta\theta_{ctr}| < \beta_1 |\Delta\theta_d|$  and  $|\epsilon_2| \leq |\Delta\theta_{ctr} - \Delta\theta_d| < \beta_2 |\Delta\theta_d|$



(see Section 2), then the stability conditions (9) of Theorem 2.1 can be also written in the following form:

$$\frac{|\Delta\theta_{max} - \Delta\theta_{ctr}| + |\Delta\theta_{ctr} - \Delta\theta_d|}{|\Delta\theta_d|} < \alpha < 1, \quad (10)$$

Inequality (10) provides us with a tool that uses statistical data from the exploratory experiments and the convergence conditions of Theorem 2.1 to define accuracy requirements for the controller (4) design.

Once the system model, as described in Subsection 2.1, is obtained the proper controller design can start. The design is based on a fuzzy logic scheme for interpolation of empirical data. Each node of this interpolation is defined by a tuple  $(\Delta\theta_j, Q_j(\cdot))$ , where  $\Delta\theta_j$  represents a displacement that should be generated by the rectangular torque pulse  $Q_j(\cdot)$  ( $j = 1, \dots, J$ ). A control function  $\Psi(\cdot; \Delta\theta)$  is defined, such that for the interpolation nodes the following equation holds:

$$\Psi(\cdot; \Delta\theta_j) = Q_j(\cdot), \quad j = 1, \dots, J, \quad (11)$$

The control function  $\Psi(\cdot; \Delta\theta)$  is designed using the fuzzy logic approach. To do this, linguistic variables are associated with interpolation nodes  $(\Delta\theta_j, Q_j(\cdot))$ . The input linguistic variable “[DESIRED DISPLACEMENT IS  $\Delta\theta_j$ ]” is associated with displacements  $\Delta\theta_j$  and the output linguistic variable “[APPLY TORQUE PULSE  $Q_j(\cdot)$ ]” is associated with pulse shapes  $Q_j(\cdot)$ . The inference rules which map one set of the linguistic variables into another are defined as follows:

$$\text{if [DESIRED DISPLACEMENT IS } \Delta\theta_j], \quad \text{then [APPLY TORQUE PULSE } Q_j(\cdot)] \quad (12)$$

In order to fuzzify the linguistic variables, triangular membership functions  $\mu_j(\Delta\theta)$  were used (see Figure 3) such that  $\mu_j(\Delta\theta_j) = 1$ ,  $\mu_j(\Delta\theta_{j-1}) = 0$  and  $\mu_j(\Delta\theta_{j+1}) = 0$  for  $j = 1, \dots, J$ . The membership functions  $\mu_1(\Delta\theta)$  and  $\mu_J(\Delta\theta)$  have constant values equal to 1 outside the bounds of the interpolation range.

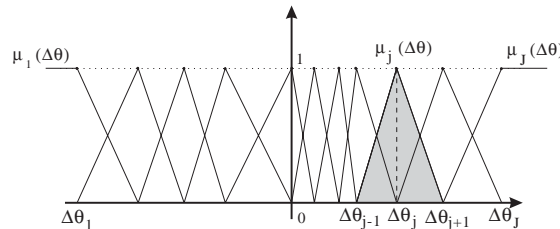


Figure 3: Schematic diagram of the fuzzification procedure

In the designed fuzzy logic controller the desired displacement  $\Delta\theta_d$  is fuzzified using the membership weights  $\mu_j = \mu_j(\Delta\theta_d)$  for the input linguistic variables [DESIRED DISPLACEMENT is  $\Delta\theta_j$ ]. In accordance with the inference rules (12), the calculated weights  $\mu_j$  are associated with the output linguistic variables [APPLY TORQUE PULSE  $Q_j(\cdot)$ ]. A “crisp” pulse shape  $\Psi(\cdot; \Delta\theta_d)$ , which is the output of the controller, is computed from the output linguistic variables using Sugeno’s defuzzification method [15]:

$$\Psi(\cdot; \Delta\theta_d) = \frac{\sum_{j=1}^J \mu_j(\Delta\theta_d) Q_j(\cdot)}{\sum_{j=1}^J \mu_j(\Delta\theta_d)}, \quad (13)$$

Note that the membership functions  $\mu_j(\Delta\theta)$  shown in Figure 3 are chosen in such a way that the denominator of (13) is always unity. Thus the controller always performs interpolation of the rectangular pulses for two closest nodes as shown in Figure 4.

The nodes  $(\Delta\theta_j, Q_j(\cdot))$  should be chosen such that the interpolation error  $\epsilon_{2n}$  in (7) satisfies the requirements of Theorem 2.1 for all desired displacements  $\Delta\theta_d$  in the given range  $[\Delta\theta_1, \Delta\theta_J]$ . This ensures the closed-loop convergence of the system. Obviously, the more interpolation nodes  $(\Delta\theta_j, Q_j(\cdot))$  are used, the smaller is the relative approximation error  $(\epsilon_2/|\Delta\theta_d|)$  and the faster is the convergence of the closed-loop system.

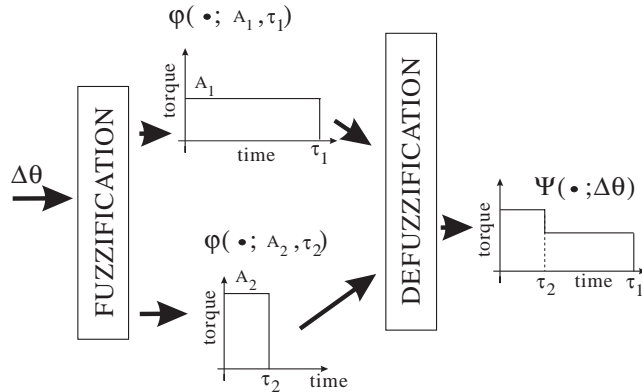


Figure 4: Schematic diagram of fuzzification and defuzzification of the pulse shapes

## 4 Experiments

### 4.1 Experimental Setup

The control strategy presented in this paper was tested experimentally using a two-link planar direct-drive (DD) manipulator designed at the Robotics and Automation Laboratory, University of Toronto [10, 11]. The arm shown schematically in Figure 5 represents a typical direct-drive mechanism that is actuated by two permanent magnet DC motors. In our

experiments only the first joint was used. The joint was actuated with a Yokogawa DMA 1050 motor and had an incremental joint encoder which had resolution 1024000 counts per revolution [18]. The current in the motor windings was controlled by a Dynaserv amplifier SD1050A-1 manufactured by Yokogawa Co. [18].

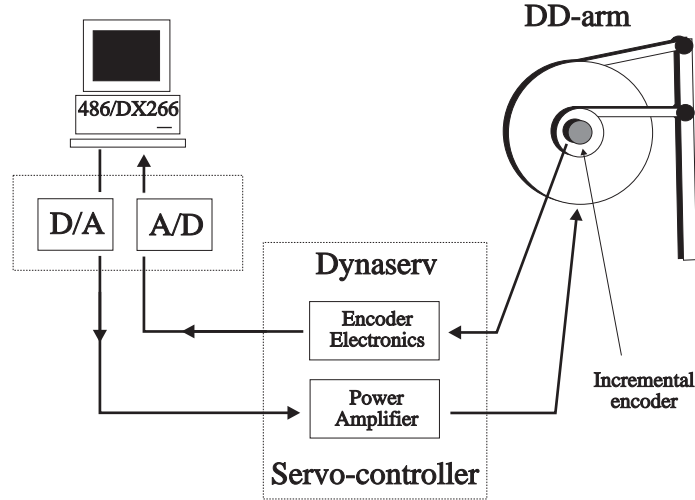


Figure 5: DD-arm setup at the Robotics and Automation Laboratory, University of Toronto

The arm was controlled with a PC-486/DX2-66 computer via Analog to Digital (A/D) and Digital to Analog (D/A) converter cards AT-MIO-16 and AT-AO-6/10 by National Instruments, respectively. The output of the D/A card was supplied to the input of the Dynaserv amplifier as a desired motor current. The control program was written in “C++”, and had the sampling time of 1 msec.

It is important to mention that conventional controllers (such as PID controllers) are capable of positioning the motor with an accuracy up to  $\pm 30$  encoder increments [10, 11]. The pulse controller presented in this paper is supposed to take over from there. Hence, the design requirement considered during the pulse controller development was that it should work within displacements of  $\pm 100$  encoder increments.

## 4.2 Model Identification Experiments

In experiments, rectangular torque pulses were sent to the motor and the time history of the motor displacement  $\Delta\theta(t)$  was recorded. The pulse amplitudes  $A$  varied from -20 Nm to 20 Nm in steps of 1 Nm, and the pulse durations  $\tau$  varied from 0 to 0.01 sec in steps of 0.001 sec. Overall, the system responses were obtained for 451 pulse shapes which correspond to different pairs  $(A, \tau)$ . For each pulse shape, 10 experiments were performed (4510 experiments

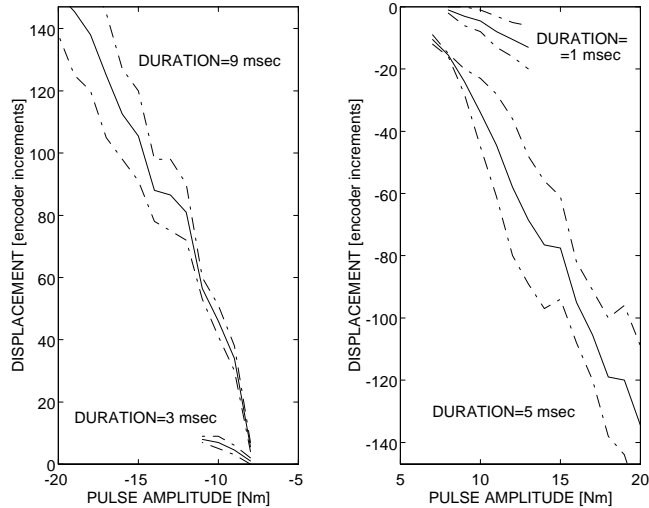


Figure 6: Results of the exploratory experiments used to design the controller

in all). The experiments were conducted for different initial positions to experimentally verify the assumption made in Subsection 2.1 that the mechanism displacement does not depend on the initial position. The experiments confirmed that this assumption holds and that the models in Section 2 are valid.

The results obtained show that it is possible to move the mechanism from 1 to 140 encoder increments in each rotational direction using rectangular pulse shape with pulse amplitude  $A$  less than 20 Nm (with the maximum motor torque being 50 Nm), and duration  $\tau$  less than 0.01 sec. Figure 1 represents a center displacement  $\Delta\theta_{ctr}$  as a function of the pulse amplitude  $A$  and the pulse duration  $\tau$ , estimated from experimental results.

The obtained experimental results also show that for any of the 451 explored rectangular torque pulses, the mechanism stops moving and comes to a steady-state in a time shorter than 0.1 sec. Thus,  $T = 0.1$  sec is used in our experiments as the controller sampling time.

### 4.3 Controller Design

The controller design follows the methodology presented in Section 3. Based on the experimental results described in Subsection 4.2, more detailed exploratory experiments were performed for the pulse durations and amplitudes presented in Table 1. The results of these experiments are shown in Figure 6. Solid lines represent the estimated center displacement  $\Delta\theta_{ctr}$  as a function of the pulse amplitude  $A$  for the specified pulse durations ( $\tau = 1$  msec,  $\tau = 3$  msec,  $\tau = 5$  msec and  $\tau = 9$  msec). Dashed lines in Figure 6 show experimentally

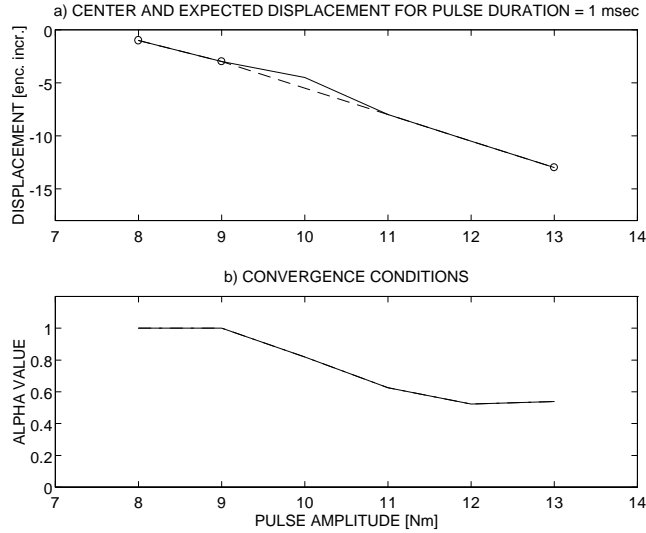


Figure 7: a) Center displacement  $\Delta\theta_{ctr}$  estimated in the experiments (solid line), fuzzy logic model (dashed line), and nodes of the fuzzy logic interpolation (circles) for the pulse duration  $\tau = 1$  msec; b) Convergence parameter  $\alpha$  for the selected nodes

$A$	[Nm]	7 $\rightarrow$ 20	8 $\rightarrow$ 13	-11 $\rightarrow$ -8	-20 $\rightarrow$ -8
$\tau$	[msec]	5	1	3	9

Table 1: Pulse parameters chosen for the exploratory experiments (“ $\rightarrow$ ” represents changing amplitude in steps of 1 Nm)

obtained upper  $\Delta\theta_{max}$  and lower  $\Delta\theta_{min}$  extremes for the random variable  $\Delta\theta$ .

The results of the experiments have been used to define the interpolation nodes ( $\Delta\theta_j$ ,  $Q_j(\cdot)$ ) of the fuzzy logic controller as points on the center displacement curves  $\Delta\theta_{ctr}$  shown in Figure 6. The interpolation nodes are selected to satisfy convergence condition (10). For example, a curve  $\Delta\theta_{ctr}(A)$  obtained for the pulse duration  $\tau = 1$  msec (see Figure 6) and its interpolation nodes which satisfy convergence condition (10) are shown in Figure 7.a. After the interpolation nodes for all four curves in Figure 6 are selected, stability conditions given by Theorem 2.1 are verified by plotting the left-hand side of the inequality (10) (stability margin) as a function of the pulse amplitude  $A$  for all four pulse durations  $\tau$ . Parameters of the rectangular torque pulses selected as the interpolation nodes for all four center displacement curves given in Figure 6 are displayed in Table 2.

Using the convergence conditions of Corollary 2.1, it is possible to determine the achievable accuracy of the closed-loop system (6) for the selected interpolation nodes. In our case, the closed-loop convergence condition (10) of Theorem 2.1 holds for  $|\Delta\theta| \geq 4$  encoder increments.

Node	1	2	3	4	5	6	7	8	9	10	11
$\Delta\theta$ [enc.inc.]	-135	-21	-13	-3	-1	0	1	5	8	34	151
$A$ [Nm]	20	8	13	9	8	0	-8	-9	-11	-9	-20
$\tau$ [msec]	5	5	1	1	1	0	3	3	3	9	9

Table 2: Interpolation nodes for the designed controller

For  $\alpha = 0.5$ , Corollary 2.1 predicts convergence of the closed-loop system in no more than 6 iterations, assuming that the initial position of the mechanism was in the range of  $\pm 128$  encoder increments from the desired final position.

#### 4.4 Closed-Loop Pulse Control Experiments

The designed controller was tested in the closed-loop experiments. The experiments were conducted as follows. The drive was first placed in a randomly selected starting position and a desired final position was given within the range of  $\pm 100$  encoder increments from the initial position. After that, the controller was activated and it sent a sequence of torque pulses to the motor until the desired position was reached with the predefined accuracy ( $\pm 4$  encoder increments which is equivalent to  $\pm 0.4 \times 10^{-6}$  m).

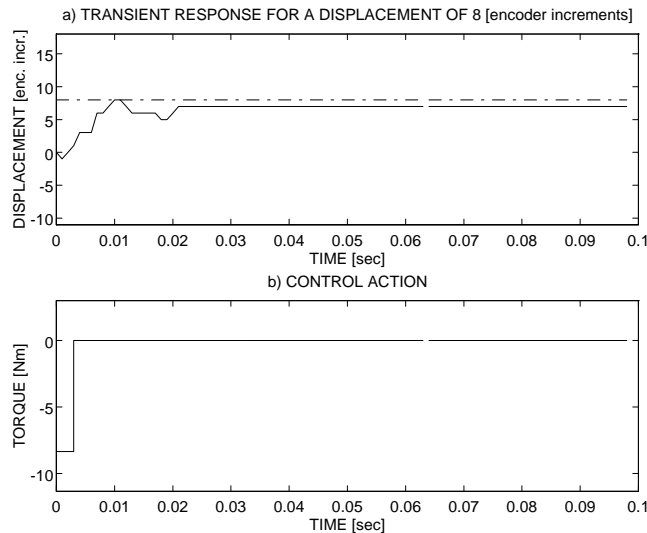


Figure 8: Control action and displacement of the arm as a function of time

The extensive testing has demonstrated that the designed controller is very robust and, generally, needs no more than six pulses to move the DD-arm to any desired position within the range of  $\pm 100$  encoder increments. This result is in-line with the Corollary 2.1 estimate in Subsection 4.3. With 100 msec sampling period between the pulses, it takes less than

0.6 sec to position the drive. In many cases, the controller is capable of positioning the drive at the desired position with a single torque pulse.

The results given in Figures 8 and 9 are obtained for the interpolation nodes given in Table 2. In Figure 8, desired displacement is 8 encoder increments and in Figure 9, -30 encoder increments. In both cases the error becomes less or equal to four encoder increments (less than  $0.4 \times 10^{-6}$  m) after 3 controller engagements.

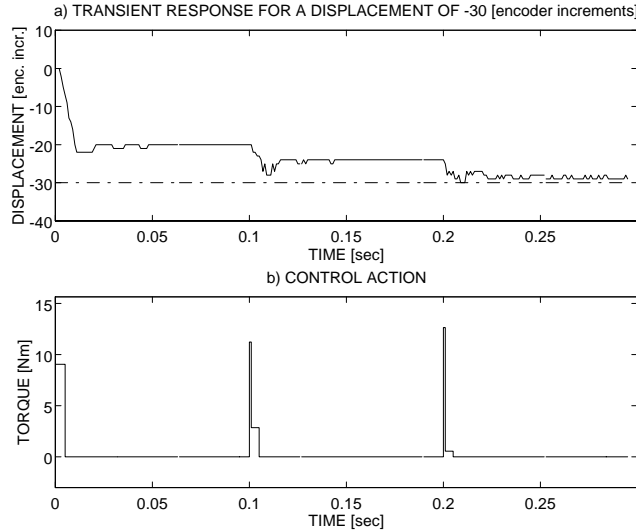


Figure 9: Control action and displacement of the arm as a function of time

## 5 Conclusions

In this paper, a new approach to very accurate positioning of mechanical devices with non-linear (stick-slip) friction is presented. The proposed controller is a sampled-data type of the controller which uses narrow torque pulses to move the mechanism to the desired position. The controller is used after a conventional controller brings the mechanism close to the desired position, to reduce or to eliminate steady-state position error created by the conventional controller. An innovative feature of the controller is that the pulse shapes generated by the controller are computed using fuzzy logic approximation of the dependence between the desired displacement and the pulse shape. A nonstandard empirically-based mathematical model of friction was developed and experimentally identified. This model takes into consideration the random variation of friction and measurement errors. The closed-loop convergence conditions for the proposed controller are derived and analyzed using this model.

In experiments with the direct drive mechanism, it was demonstrated that the proposed controller is able to achieve positioning precision close to the limits of the position encoder resolution (less than  $0.4 \times 10^{-6}$  m) under all conditions.

## References

- [1] Armstrong B., Control of Machines with Friction, Kluwer Academic Publishers, Boston, USA, 1991.
- [2] Dupont P.E., "Avoiding Stick-Slip in Position and Force Control Through Feedback," *Proc. of the IEEE Int. Conf. on Robotics and Automation*, 1991, pp.1470-1475.
- [3] Canudas de Wit C., Adaptive Control for Partially Known Systems, Elsevier, Boston, USA, 1988.
- [4] Gorinevsky, D., Torfs, D, and Goldenberg, A.A. "Learning Approximation of Feedforward Control Dependence," *IEEE Tr. on Robotics and Automation*, Vol.13, No.4, 1997, pp.567-581.
- [5] Gorinevsky D., and Vukovich G., "Control of Flexible Spacecraft Using Nonlinear Approximation of Input Shape Dependence on Reorientation Maneuver Parameters," *Proc. of the 13th World Congress of IFAC*, San Francisco, CA, Vol.P, pp.285-290.
- [6] Gumbel E.J., Statistics of Extremes, Columbia University Press, New York, USA, 1966.
- [7] Higuchi T., and Hojjat Y., "Application of Electromagnetic Impulsive Force to Precise Positioning," *Proc. of the IFAC 10th Triennial World Congress*, 1987, pp.283-288.
- [8] Hojjat Y., and Higuchi T., "Positioning Mechanism and Fundamental Experiment," *Int. J. Japan Soc. Precision Eng.*, Vol.25(1), 1991, pp.39-44.
- [9] Lee H.S. and Tomizuka M., "Robust Motion Controller Design for High-Accuracy Positioning Systems," *IEEE Tr. On Industrial Electronics*, Vol.43, No.1, 1997, pp.48-55.
- [10] Liu G.J., and Goldenberg A.A., "Comparative Study of Robust Saturation Control of Robot Manipulators: Analysis and Experiments," *International Journal of Robotics Research*, Vol.15, No.5, 1996, pp.473-491.
- [11] Popović M.R., Shimoga K.B., and Goldenberg A.A., "Modeling and Compensation of Friction in Direct-Drive Robotic Arms," *Proc. of the JSME Int. Conf. on Advanced Mechatronics*, 1993, pp.810-815.
- [12] Popović M.R., Gorinevsky D.M., and Goldenberg A.A., "Fuzzy Logic Controller for Accurate Positioning of Direct-Drive Mechanism Using Force Pulses," *Proc. of the IEEE Int. Conf. on Robotics and Automation*, Vol. 1, 1995, pp.1166-1171.
- [13] Popović M.R., Friction Modeling and Control, PhD Thesis, University of Toronto, Canada, 1996.
- [14] Southward S.C., Radcliffe C.J., and MacCluer C.R., "Robust Nonlinear Stick-Slip Friction Compensation," *Proc. of the ASME Winter Annual Meeting*, 1990, ASME paper No. 90-WM/DAC-8, 7 pages.
- [15] Takagi T., and Sugeno M., "Fuzzy Identification of Systems and its Applications to Modeling and Control," *IEEE Tr. on Syst. Man and Cybernetics*, Vol.15, 1985, pp.116-132.
- [16] Yang S., and Tomizuka M., "Adaptive Pulse Width Control for Precise Positioning Under the Influence of Stiction and Coulomb Friction," *Trans., ASME, J. Dynam. Syst. Meas. and Control*, September 1988, Vol.110, No.3, pp.221-227.
- [17] Yao B., Al-Majed M. and Tomizuka M., "High-Performance Robust Motion Control of Machine Tools: An Adaptive Robust Control Approach and Comparative Experiments," *IEEE Tr. On Mechatronics*, Vol.2, No.2, 1997, pp.63-76.
- [18] Yokogawa, Product Literature on DMA and DMB Series Direct-Drive Motors, Yokogawa Co. of America, Lake Geneva, MI, 1989.